

Effect of Subaperture Beamforming on Phase Coherence Imaging

Hideyuki Hasegawa and Hiroshi Kanai

Abstract—High-frame-rate echocardiography using unfocused transmit beams and parallel receive beamforming is a promising method for evaluation of cardiac function, such as imaging of rapid propagation of vibration of the heart wall resulting from electrical stimulation of the myocardium. In this technique, high temporal resolution is realized at the expense of spatial resolution and contrast. The phase coherence factor has been developed to improve spatial resolution and contrast in ultrasonography. It evaluates the variance in phases of echo signals received by individual transducer elements after delay compensation, as in the conventional delay-and-sum beamforming process. However, the phase coherence factor suppresses speckle echoes because phases of speckle echoes fluctuate as a result of interference of echoes. In the present study, the receiving aperture was divided into several subapertures, and conventional delay-and-sum beamforming was performed with respect to each subaperture to suppress echoes from scatterers except for that at a focal point. After subaperture beamforming, the phase coherence factor was obtained from beamformed RF signals from respective subapertures. By means of this procedure, undesirable echoes, which can interfere with the echo from a focal point, can be suppressed by subaperture beamforming, and the suppression of the phase coherence factor resulting from phase fluctuation caused by such interference can be avoided. In the present study, the effect of subaperture beamforming in high-frame-rate echocardiography with the phase coherence factor was evaluated using a phantom. By applying subaperture beamforming, the average intensity of speckle echoes from a diffuse scattering medium was significantly higher (−39.9 dB) than that obtained without subaperture beamforming (−48.7 dB). As for spatial resolution, the width at half-maximum of the lateral echo amplitude profile obtained without the phase coherence factor was 1.06 mm. By using the phase coherence factor, spatial resolution was improved significantly, and subaperture beamforming achieved a better spatial resolution of 0.75 mm than that of 0.78 mm obtained without subaperture beamforming.

I. INTRODUCTION

ECHOCARDIOGRAPHY is a widely used modality for diagnosis of the heart. Because of the temporal resolution, which is much better than those of computed tomography (CT) and magnetic resonance imaging (MRI), echocardiography is indispensable for evaluation of cardiac function in clinical situations. In addition to the morphological observation of cross-sectional images of the heart based on ultrasonography, ultrasonic meth-

ods for measurements of the myocardial strain and strain rate [1]–[4] have been developed and used for evaluation of cardiac function. Also, it has been recently reported that the propagation of myocardial electrical excitation, which has been visualized by ultrasonic measurement of electrical-stimulation-induced myocardial motion, can be observed by further increasing the temporal resolution in echocardiography [5], [6]. The measurement of such propagation phenomenon would be useful for detection of a site of myocardial infarction. The electrical excitation propagates in Purkinje fibers and ventricular muscle at typical velocities of 2 to 4 m/s [7], [8], and the corresponding propagation velocities of myocardial contraction of 0.9 to 4 m/s have been measured by ultrasound [5]. In those cited studies, frame rates of several hundred hertz, which were much higher than the several tens of hertz in conventional echocardiography, were realized by sparse scan (low density of scan lines) and ECG gating (requiring several cardiac cycles to obtain an entire image).

To realize high-frame-rate echocardiography without decreasing the density of scan lines and ECG gating, Lu *et al.* used plane waves in transmission to illuminate a wider region by one emission and to reconstruct an image of the illuminated region [9] based on diffraction tomography [10]–[12]. Recently, a diverging beam, which emulates a spherical wave from a virtual point source behind an array, has been found to be usable to illuminate an even wider region than a plane wave, and diverging beam transmission and parallel receive beamforming have been shown to be feasible in high-frame-rate echocardiography [13]–[17].

Recent developments in high-frame-rate ultrasonography commenced with linear arrays [18]–[21]. Using parallel beamforming, temporal resolution has been significantly improved, but spatial resolution was degraded by the use of unfocused transmit beams. To improve spatial resolution, coherent plane-wave compounding has been introduced [22]. In this technique, beamformed RF signals at the same spatial point, which were obtained by transmitting plane waves from different directions, were coherently averaged. By means of this procedure, the synthesized point spread function became narrower (i.e., had better spatial resolution) than those formed by individual transmissions. In the case of a linear array, the size of the aperture is large, i.e., the width of a plane wave is large, and plane waves can be compounded coherently even when the steering angle is relatively large. On the other hand, in echocardiography using a phased array, ultrasound must be insonified from a narrow acoustic window between ribs and, thus, the size of the aperture, corresponding to the

Manuscript received February 27, 2014; accepted July 31, 2014.

The authors are with the Graduate School of Biomedical Engineering and the Graduate School of Engineering, Tohoku University, Sendai, Japan (email: hasegawa@ecei.tohoku.ac.jp).

DOI <http://dx.doi.org/10.1109/TUFFC.2014.006365>

width of a plane wave, is limited. Under such conditions, it is difficult to compound plane waves at different steering angles, and the effect of compounding is degraded.

To improve spatial resolution and contrast in ultrasonography, the minimum variance beamforming method has been developed [23]. This method improves the spatial resolution significantly by minimizing the power of echo signals coming from undesired directions (i.e., except for the focal point). In minimum variance beamforming, Synnevåg also introduced sub-array averaging for controlling the trade-off between the robust solution and the spatial resolution [24]. This method requires calculation of the covariance matrix of the complex echo signals received by individual transducer elements after delay compensation as in conventional delay-and-sum beamforming process, and the inverse matrix of the covariance matrix must be obtained. Therefore, although minimum variance beamforming is a promising method for improvement of spatial resolution, it is computationally intensive.

There is another technique, namely, the phase coherence factor (PCF) [25], which would also be effective for improvement of spatial resolution and contrast in high-frame-rate echocardiography. However, speckle echoes tend to be suppressed by the phase coherence factor, whereas strong echoes tend to be enhanced. In echocardiography, specular reflection from valves and the interface between the heart wall and blood should be visualized, but speckle echoes from the inside of the heart wall should also be visualized. Therefore, in the present study, a strategy for use of the phase coherence factor was proposed for avoiding suppression of speckle echoes from a diffuse scattering medium.

II. PRINCIPLES

A. Phase Coherence Factor

The phase coherence factor [25] is used for weighting beamformed RF echoes to improve spatial resolution and contrast in ultrasonography. The weight is determined by evaluating the variance in phases of ultrasonic RF echoes received by individual transducer elements. The phase variance is evaluated after delay compensation as in a conventional delay-and-sum beamforming process. When an echo comes from a scatterer exactly located at a focal point of the beamformer, echoes received by individual elements are perfectly aligned after the application of delay compensation and, thus, the phase variance among elements would be zero, corresponding to high phase coherence factor (maximum is 1). Because of this property of the phase coherence factor, echoes from spatial points except for a focal point will be suppressed because of focusing errors resulting in increased phase variance, and spatial resolution and contrast will be improved.

To obtain phases of echo signals received by individual elements, in the present study, for computational efficiency, the complex signal $g_i(t)$ of the echo signal $s_i(t)$ received

by the i th element ($i = 1, 2, \dots, N$) was obtained using the short-time Fourier transform with respect to the ultrasonic center frequency f_0 instead of the analytic signal obtained by the Hilbert transform. The short-time Fourier transform was used with a Hann window of $0.512 \mu\text{s}$ in length. Under this condition, the first nulls of the power spectrum of the Hann window in estimation of the Fourier coefficient at the ultrasonic center frequency of 3 MHz were located at -0.125 and 6.25 MHz. Although a shorter window can increase the frequency bandwidth of its main lobe, components at negative frequencies would be included to estimate the Fourier coefficient at 3 MHz. Therefore, in the present study, one of the first nulls was placed close to 0 MHz. By estimating the Fourier coefficient only at the ultrasonic center frequency, the computational load was significantly lower than the Hilbert transform. In delay compensation in conventional delay-and-sum beamforming, subsample time delay τ_s was compensated by multiplying the estimated complex signal $g_i(t)$ by $\exp(j2\pi f_0 \tau_s)$. The phase coherence factor PCF was evaluated using the phase ϕ_i of $g_i(t) \cdot \exp(j2\pi f_0 \tau_s)$. However, the estimated phases ϕ_i have discontinuity when the estimated phase value crosses the $+\pi$ and $-\pi$ boundary, despite the fact that phases close to $\pm\pi$ are similar. To avoid this pitfall, the auxiliary phase ϕ_i^A was also obtained, where $+\pi$ was added to ϕ_i if $\phi_i < 0$ and $-\pi$ is added if $\phi_i > 0$. The standard deviations σ_1 and σ_2 across the receiving aperture were estimated with respect to ϕ_i and ϕ_i^A , respectively, and the smaller standard deviation (σ_1 or σ_2) was used as the standard deviation σ of the phases of echoes received by individual elements. Using the estimated standard deviation σ , the coherence factor PCF was estimated as

$$\text{PCF} = 1 - \frac{\sigma}{\sigma_0}, \quad (1)$$

where σ_0 is the nominal standard deviation of $\pi/3^{1/2}$ of a uniform distribution between $-\pi$ and π [25].

B. Problem in Conventional Phase Coherence Imaging

One important consideration in this procedure is that echoes from multiple scatterers should overlap in the signal received by each element. Let us consider the case in which an echo from a scatterer exactly located at a focal point of a beamformer is much stronger than other echoes, namely, out-of-focus echoes. Fig. 1(1-a) shows RF echoes received by individual elements and their phases obtained after delay compensation in a conventional delay-and-sum beamforming process. The red dashed lines in Fig. 1 show the focal point. In such a case, the contribution of out-of-focus echoes is negligible because the echo from the focal point is dominant, and phases of signals received by individual elements reflect the phase of the dominant echo from the focal point. Therefore, the phases are similar at the focal point and the phase variance is low, i.e., the phase coherence factor is high.

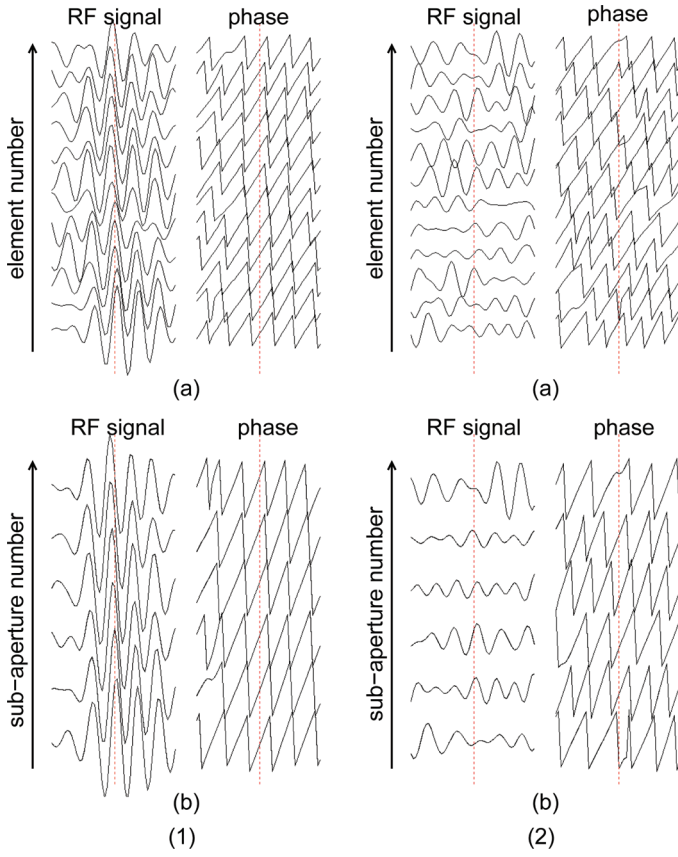



Fig. 1. RF echoes and their phases obtained from (1) a strong scatterer and (2) a weak scatterer; RF echoes and their phases are obtained by individual (a) elements and (b) subapertures. 

On the other hand, when an echo from a focal point is weak, e.g., echoes from a diffuse scattering medium, contributions of out-of-focus echoes cannot be negligible. Fig. 1(2-a) shows RF echoes from a diffuse scattering medium and their phases. As can be seen in Fig. 1(2-a), RF echoes are not aligned even after delay compensation because out-of-focus echoes are not negligible and interfere with the echo from the focal point. In such a case, the phase variance would be high, i.e., a low phase coherence factor, even when a weak echo coming from the focal point exists.

C. Strategies for Avoiding Suppression of Speckle Echoes in Phase Coherence Imaging

For avoiding undesirable suppression of weak echoes from a diffuse scattering medium, in the present study, some strategies for evaluation of the phase variance were examined, as described subsequently.

1) *Controlled PCF* [25]: A method for avoiding suppression of speckle echoes, which should be mentioned first, is to weaken the effect of the phase coherence factor by introducing a control parameter γ as follows [25]:

$$\text{PCF}^\gamma = 1 - \frac{\gamma}{\sigma_0} \sigma. \quad (2)$$

In the present study, a controlled phase coherence factor $\text{PCF}^{0.5}$ at $\gamma = 0.5$ was examined.

2) *PCF With Subaperture Beamforming* [26]: In the case of a diffuse scattering medium, the interference between an echo from a focal point and out-of-focus echoes significantly influences the phase estimated from the echo signal received by each element. Therefore, out-of-focus echoes must be suppressed to estimate the phase of an echo from the focal point. To suppress the contributions of out-of-focus echoes, a receiving aperture consisting of N elements was divided into M subapertures. Each subaperture performs conventional delay-and-sum beamforming with respect to an assigned focal point. By subaperture beamforming, echoes from scatterers except for that at the focal point can be suppressed. Figs. 1(1-b) and 1(2-b) show RF echoes and their phases obtained after subaperture beamforming. For the strong echo from the focal point [Fig. 1(1-b)], there is no significant change in the RF echoes and phases at the focal point between pre- and post-subaperture beamforming because out-of-focus echoes are negligible. On the other hand, in the case of the weak echo from a diffuse scattering medium shown in Fig. 1(2-b), there is a significant change in RF echoes between pre- and post-subaperture beamforming. By subaperture beamforming, an echo from the focal point was enhanced, and the differences in phases at the focal point became smaller than those before subaperture beamforming.

In the present study, non-overlapping and overlapping subapertures were examined. Hyun *et al.* showed that subaperture beamforming could be used for efficient calculation of spatial coherence in the use of a 2-D matrix array [27]. They showed that the short-lag spatial coherence estimated without subaperture beamforming showed the best performance but subaperture beamforming led to no significant degradation of the performance. Overlapping subapertures were used in [28] for improving estimation of aberration in received ultrasonic echoes.

In the case of non-overlapping subapertures, each subaperture consists of N/M elements. On the other hand, the number of subapertures and the number of elements in each subaperture can be assigned independently. However, in comparison between non-overlapping and overlapping subapertures, the same number of elements in each subaperture was used and the number of subapertures was set at $N - M + 1$ (the subaperture was shifted by one element) in the case of overlapping subapertures. The phase coherence factor was estimated using the phases of the subaperture output signals based on (2).

3) *PCF With Reduced Number of Elements*: The estimation of the phase coherence factor with subapertures beamforming significantly reduces the number of phase data for estimating the phase variance. Using a smaller number of phase data increases the variance in the estimated phase variance (see appendix). The increased variance in estimation of the phase variance would increase the case in which the phase variance evaluated from echoes from

diffuse scattering medium becomes low. This means that speckle echoes from a diffuse scattering medium are more likely visualized compared with the case in which a larger number of phase data are used. To examine the effect of the number of phase data on phase coherence imaging, in the present study, the phase coherence factor was also estimated using a smaller number of elements (and, therefore, phase data). The number of elements corresponds to the number of subapertures in the non-overlapping case.

III. EXPERIMENTAL RESULTS

A. Basic Experiments Using Phantom

In the present study, a custom-made ultrasound system (RSYS0002, Microsonic, Tokyo, Japan), which enables 96-channel simultaneous transmit and is able to acquire ultrasonic RF echoes from 96 elements, was used with a commercial 3.75-MHz phased array probe (UST-52101, Hitachi-Aloka, Tokyo, Japan). The total number of elements and the element pitch of the phased array probe were $N = 96$ and 0.2 mm, respectively. Ultrasonic echoes received by individual elements were sampled at 31.25 MHz at 12-bit resolution for off-line processing (receive beamforming, estimation of phase coherence factor, etc.). An ultrasound imaging phantom (model 54GS, Computerized Imaging Reference Systems Inc., Norfolk, VA) was used for evaluation of spatial resolution and effects of subaperture beamforming on speckle echoes from a diffuse scattering medium. The phantom includes fine wires and cyst phantoms in a diffuse scattering medium.

Fig. 2(a) shows a B-mode image of the phantom obtained by parallel receive beamforming described in [14] with transmissions of diverging waves in 15 directions. The virtual point source was 100 mm behind the array, and the angular interval between transmit beams was 6° . The lateral amplitude profile of the B-mode image at a range distance of 42 mm is shown in Fig. 3. To evaluate spatial resolution, the width at half-maximum of the amplitude profile of an echo from a wire was calculated from the data shown in Fig. 3. The width at half-maximum w_l was estimated to be 1.06 mm. For consideration of the effects of subaperture beamforming on speckle echoes from a diffuse scattering medium, ratio r_a between the peak amplitude of an echo from a wire to the average echo amplitude in the diffuse scattering medium (corresponding to the region indicated by lateral angle θ of $-45^\circ < \theta < -5^\circ$ in Fig. 3) was evaluated. Also, the mean over standard deviation μ/σ of the echo amplitude profile in $-45^\circ < \theta < -5^\circ$ was obtained for evaluation of image blurring. The ratio r_a and mean over standard deviation μ/σ were evaluated to be -32.3 dB and 7.2 dB, respectively, for parallel beamforming without the phase coherence factor. In the B-mode image obtained without the phase coherence factor, speckle echoes can be observed, but the image is blurred by undesired signals, such as electrical noise and

echoes originating from side lobes, which would increase the mean μ of echo amplitudes.

Fig. 2(b) shows a B-mode image of the phantom obtained with the phase coherence factor with no subaperture beamforming. In Fig. 2(b), although the lateral spatial resolution is improved by using the phase coherence factor, speckle echoes in a diffuse scattering medium are significantly suppressed. Lateral spatial resolution w_l was 0.78 mm. Amplitude ratio r_a and mean over standard deviation μ/σ were evaluated to be -48.7 dB and -0.3 dB, respectively. The mean over standard deviation μ/σ was decreased because the speckle echoes were more visualized by the phase coherence factor and the standard deviation σ was increased.

Figs. 2(c), 2(d), 2(e), and 2(f) show B-mode images obtained with controlled coherence factor, coherence factors estimated with non-overlapping subapertures, reduced number of elements, and overlapping subapertures, respectively. With respect to the controlled phase coherence factor, the spatial resolution w_l was 0.92 mm. The amplitude ratio r_a and mean over standard deviation μ/σ were -36.5 dB and 6.34 dB, respectively. Although the increased r_a of -36.5 dB shows the enhancement of speckle echoes, the increased w_l and μ/σ show the degraded spatial resolution and image blurring, respectively.

Then, phase coherence factors obtained with non-overlapping subapertures and reduced number of elements were compared. The number of elements in each non-overlapping subaperture was N/M (where M is the number of subapertures and N is the total number of elements). In Fig. 2(d), $M = 4$. In Fig. 2(e), the number of elements used for estimation of the phase coherence factor was 4, where each element was located at the position corresponding to the center of each of the non-overlapping subapertures in Fig. 2(d). In Fig. 2(d), spatial resolution w_l , amplitude ratio r_a , and mean over standard deviation μ/σ are 0.75 mm, -39.9 dB, and 3.6 dB, respectively. In Fig. 2(e), spatial resolution w_l , amplitude ratio r_a , and mean over standard deviation μ/σ are 0.77 mm, -39.4 dB, and 5.3 dB, respectively. In terms of speckle-echo visualization, non-overlapping subaperture and reduced number of elements showed similar performances. However, the phase coherence factor estimated with non-overlapping subapertures achieved better spatial resolution (smaller w_l) with less blurring (lower μ/σ). Figs. 4(a), 4(b), and 4(c) summarize estimated spatial resolution $\{w_l\}$, amplitude ratios $\{r_a\}$, and means over standard deviation, $\{\mu/\sigma\}$, respectively.

As shown in Fig. 4(a), the spatial resolution w_l evaluated from an echo from a fine wire (strong scatterer) was further improved by subaperture beamforming. A strong echo from a strong scatterer located at a focal point is also interfered by weak echoes from diffuse scattering medium, which is surrounding the strong scatterer. Although the effect of such interference is smaller than that between echoes both from weak scatterers in diffuse scattering medium, the phase variance estimated with respect to the

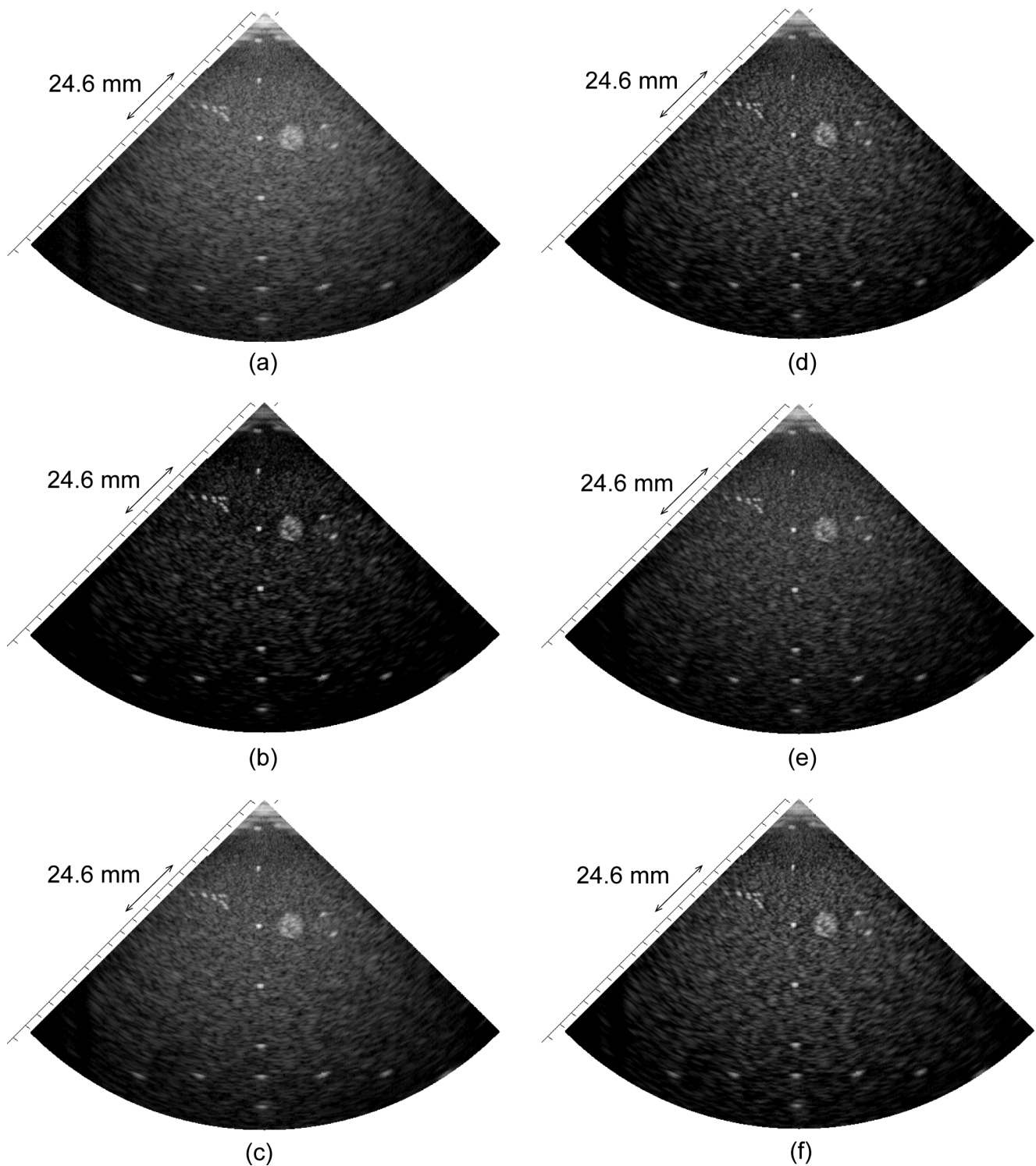


Fig. 2. B-mode images of phantom: (a) without the phase coherence factor, (b) with the conventional phase coherence factor, (c) with the controlled phase coherence factor ($\gamma = 0.5$), (d) with the phase coherence factor with 4 non-overlapping subapertures (24 elements/subaperture), (e) with the phase coherence factor estimated by 4 elements, and (f) with the phase coherence factor with 73 overlapping subapertures (24 elements/subaperture).

strong echo from the focal point would increase, which leads to suppression of the peak amplitude (at the focal point) of the strong echo. As a result, the spatial resolution, which was evaluated as the width at half-maximum of the echo amplitude, was degraded slightly when the phase coherence factor was estimated without subaperture beamforming (corresponding to a reduced number

of elements). Using subaperture beamforming, such weak echoes interfering with the strong echo at the focal point were suppressed, and the spatial resolution was improved.

As shown in Fig. 4(b), amplitude ratios $\{r_a\}$, which are similar at all numbers of subapertures and number of elements, show that phase coherence factors estimated with non-overlapping subapertures and reduced number of ele-

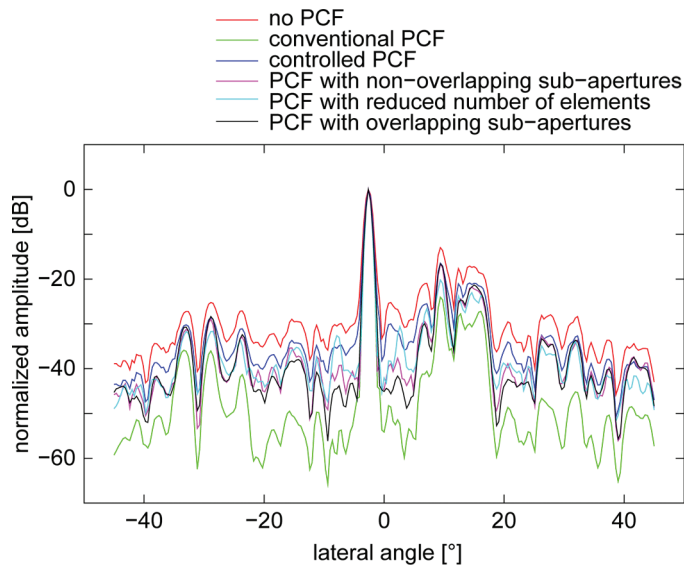


Fig. 3. Lateral amplitude profiles of B-mode images at range distance of 42 mm. Profiles were obtained without phase coherence factor (PCF), with conventional PCF, with controlled PCF, with PCF obtained by 4 non-overlapping subapertures (24 elements/subaperture), with PCF obtained by reduced number of elements (4 elements), and with PCF obtained by 73 overlapping subapertures (24 elements/subaperture).

ments realized similar levels of speckle-echo visualization. However, it should be noted that the average echo amplitude is also increased by random noise, such as electrical noise. This result suggests that the average echo amplitude in a diffuse scattering medium depends on the number of data used for estimation of the phase coherence factor. By reducing the number of data used for estimation of the phase coherence factor, the variance in estimation of the phase variance becomes higher, as described in the appendix, and the difference between the phase coherence factor of the coherent echo and that of the incoherent component, e.g., echoes from diffuse scattering medium, electrical noise, etc., is possibly decreased more. As a result, the increase in the difference between relative magnitudes of the coherent echo and the incoherent component was suppressed by decreasing the number of data used for estimation of the phase coherence factor.

In an ultrasound imaging, echo speckles increase the standard deviation in the echo amplitude profile. On the other hand, random noise, such as electrical noise, leads to noisy images; i.e., the mean of the echo amplitude profile in an ultrasound image increases. In Fig. 4(c), the mean over standard deviation μ/σ obtained with subaperture beamforming was lower than that obtained with reduced number of elements (without subaperture beamforming). This means that subaperture beamforming realizes more enhancement of speckle echoes. As shown in Fig. 4(b), the average echo amplitudes in diffuse scattering medium are similar, and more enhancement of speckle echoes (not random noise) is possible by the phase coherence factor obtained with subaperture beamforming.

Therefore, by evaluating the mean over standard deviation, it can be confirmed whether speckle echoes or

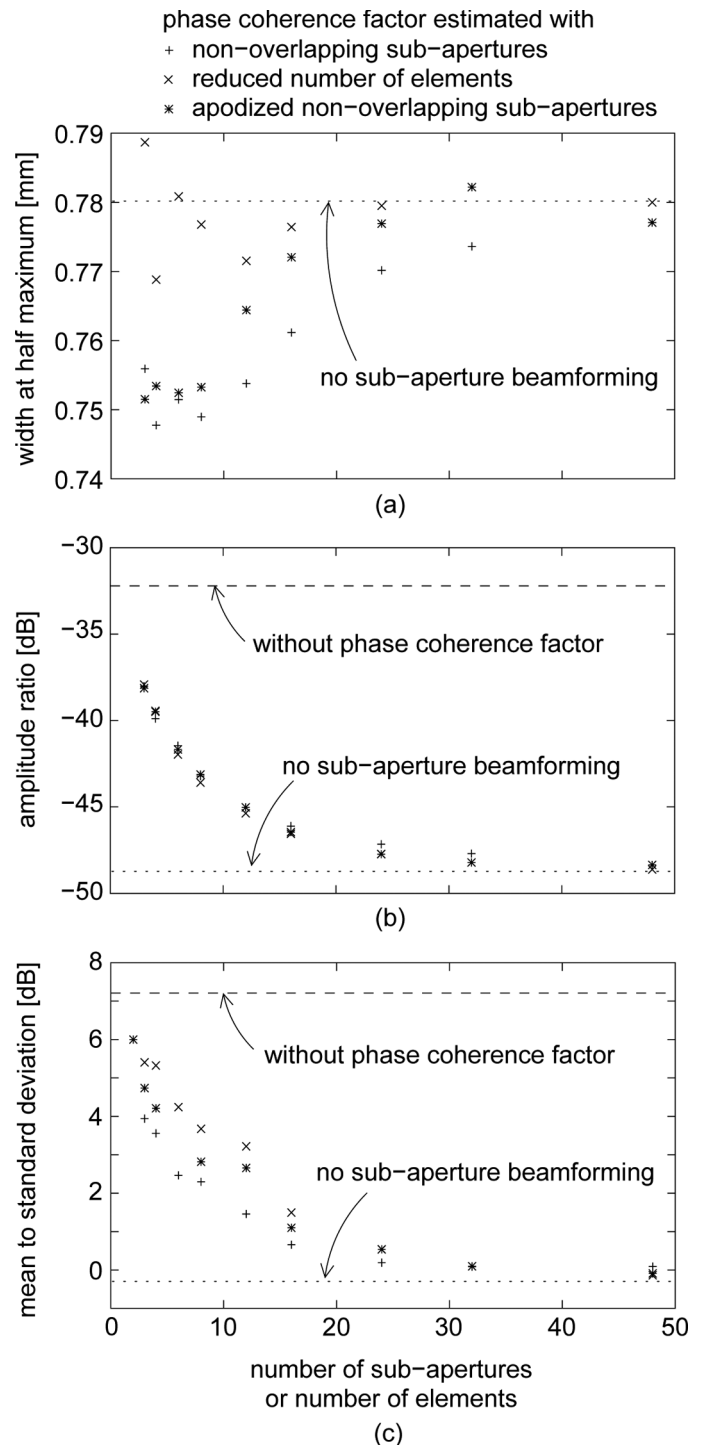


Fig. 4. Basic experimental results obtained with phase coherence factors, which were estimated with non-overlapping subapertures and reduced number of elements. (a) Lateral widths at half-maxima $\{w_l\}$ of echo amplitude profiles (w_l obtained without the phase coherence factor (PCF) was much larger (1.06 mm) and not indicated in the figure). (b) Amplitude ratios $\{r_a\}$. (c) Mean to standard deviation of echo amplitude profile.

random noise is enhanced. In Fig. 4(c), the mean over standard deviation μ/σ obtained with subaperture beamforming was lower than that obtained with reduced number of elements (without subaperture beamforming). This means that subaperture beamforming realizes more sup-

pression of random noise. As shown in Fig. 4(b), the average echo amplitudes in diffuse scattering medium are similar, and more enhancement of speckle echoes (not random noise) is possible by the phase coherence factor obtained with subaperture beamforming.

In Fig. 4, spatial resolution w_l , amplitude ratio r_a , and mean over standard deviation μ/σ are also evaluated with respect to ultrasound images obtained using Hann apodization in each subaperture beamforming. Subaperture apodization controls the effect of suppression of out-of-focus echoes by changing the effective size of subaperture, which is similar to controlling the effect of the coherence factor by changing the filter coefficient (corresponding to the cut-off direction of arrival) in [29]. Subaperture apodization weakens the effect of subaperture beamforming because apodization reduces the effective subaperture size. As shown in Fig. 4, although the phase coherence factor obtained with apodized subapertures also improves speckle-echo visualization, as indicated by the amplitude ratio r_a , the spatial resolution w_l and the mean over standard deviation μ/σ are degraded by subaperture apodization.

In Fig. 4, it is shown that subaperture beamforming is useful for improving the spatial resolution and visualization of speckle echoes. However, subapertures do not overlap, and the number of subapertures are limited, particularly at a large number of elements in each subaperture. To evaluate the effect of the number of subapertures, the results were also obtained with non-overlapping and overlapping subapertures, as shown in Fig. 5.

Using overlapping subapertures, the spatial resolution w_l was degraded at a large number of elements in each subaperture. In the case of overlapping subapertures with a large number of elements, the information from subapertures are not independent, and the echo signals from elements, which are located around the center of the total aperture, are used many times (corresponding to the number of subapertures) to obtain the phase coherence factor. This can be considered as the aperture data being apodized by a weighting function whose weight is high around the central of the aperture when we regard the beamformed signals from respective subapertures as the signals from array elements. The effective aperture size of the array is reduced by such apodization and, therefore, the lateral spatial resolution is degraded, as shown in Fig. 5(a), using overlapping subapertures. Also, for random noise, the randomness among noises contained in the signals from subapertures is degraded using overlapping subapertures even when noises contained in the signals from individual elements are random. As a result, the effect of averaging of the signals from subapertures on suppression of random noise is degraded, and the mean over standard deviation μ/σ is larger than that obtained with non-overlapping subapertures.

In summary, subaperture beamforming in estimation of the phase coherence factor can improve the spatial resolution and speckle-echo visualization, and the effect of the phase coherence factor can be controlled in various ways, such as introducing a control parameter, re-

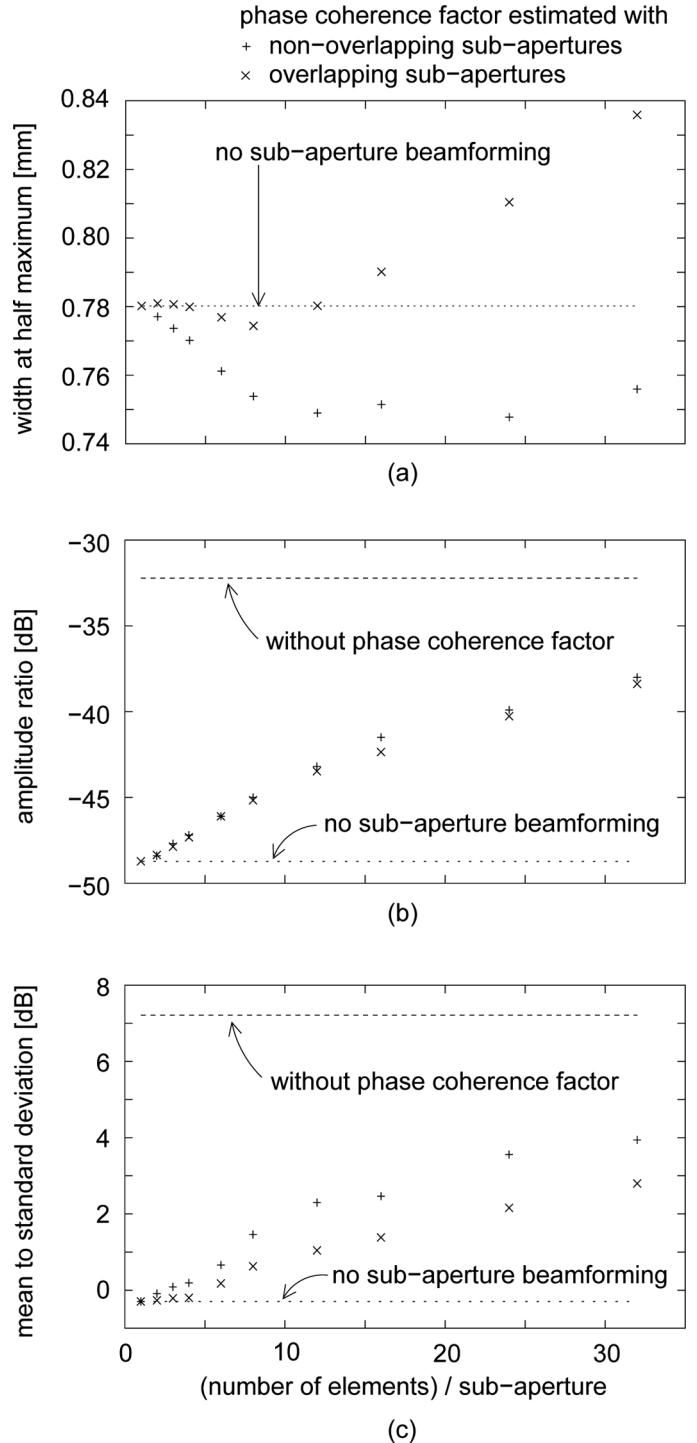


Fig. 5. Basic experimental results obtained with phase coherence factors, which were estimated with non-overlapping and overlapping subapertures. (a) Lateral widths at half-maxima $\{w_l\}$ of echo amplitude profiles (w_l obtained without the phase coherence factor (PCF) was much larger (1.06 mm) and not indicated in the figure). (b) Amplitude ratios $\{r_a\}$. (c) Mean to standard deviation of echo amplitude profile.

ducing the number of elements, subaperture apodization, and using overlapping subapertures. Introducing a control parameter, reducing the number of elements, and subaperture apodization improve speckle-echo visualization but degrade the spatial resolution. The use of overlapping subapertures slightly degrades the spatial resolution

but improves speckle-echo visualization (higher amplitude ratio r_a) compared with the use of non-overlapping subapertures, particularly at a large number of elements in each subaperture. Therefore, the phase coherence factor obtained with overlapping subapertures might be a useful strategy. However, the use of overlapping subapertures requires a significant additional computational cost, and the phase coherence factor obtained with non-overlapping subapertures shows good performance and seems effective for improvement of the spatial resolution while preserving speckle echoes.

B. In Vivo Measurement of Human Heart

Fig. 6(a) shows a B-mode image of the heart of a 26-year-old healthy male. By weighting beamformed RF signals using the conventional phase coherence factor, undesirable signals in the cardiac lumen are suppressed, as shown in Fig. 6(b). However, speckle echoes inside the heart wall are also suppressed significantly.

Figs. 6(c), 6(d), 6(e), and 6(f) show B-mode images obtained with controlled coherence factor, coherence factors estimated with 4 non-overlapping subapertures, reduced number of elements of 4, and 73 overlapping subapertures (sizes of subapertures were same as those of 4 non-overlapping subapertures), respectively. By introducing the control parameter, the effect of the phase coherence factor was weakened, and speckle echoes inside the heart wall could be visualized. However, undesired echoes in the cardiac lumen were hardly suppressed.

As can be seen in Figs. 6(d), 6(e), and 6(f), undesirable echoes in the cardiac lumen could be suppressed by the phase coherence factors estimated with non-overlapping subapertures, reduced number of elements, and overlapping subapertures while preserving speckle echoes inside the heart wall. However, there are slightly more undesirable signals in the cardiac lumen in the case of the reduced number of elements shown in Fig. 6(e).

As shown in Figs. 6(d) and 6(f), subaperture beamforming realizes good performance in suppressing undesirable signals while preserving speckle echoes inside the heart wall, whereas the larger speckle size in Fig. 6(f) shows the slight degradation of the spatial resolution by overlapping subapertures as described in Section III-A. From these results, it was also shown in the *in vivo* measurement that subaperture beamforming improves visualization of speckle echoes in phase coherence imaging.

IV. DISCUSSION

As described in the present paper, the phase coherence factor is very useful for improvement of spatial resolution and contrast in high-frame-rate echocardiography. However, the phase coherence factor suppresses speckle echoes significantly, and, therefore, a strategy for avoiding suppression of speckle echoes has been proposed. In the present study, the phase coherence factor was obtained

with subaperture beamforming to suppress the influence of out-of-focus echoes.

As shown in Fig. 4(a), the spatial resolution w_l evaluated from an echo from a fine wire (strong scatterer) was further improved by subaperture beamforming. For interpretation of such slight improvement of the lateral spatial resolution owing to subaperture beamforming, we have conducted a simple simulation experiment. In this simulation, it was assumed that an ultrasonic echo from a point target was received by 96 elements at element pitches of 0.2 mm. The point scatterer was located at 40 mm in range distance and 0° in lateral direction. The ultrasonic center frequency was set at 3 MHz and a Hanning envelope with 3 cycles at the ultrasonic center frequency was assumed. White noise was added to the simulated ultrasonic signals at a signal-to-noise ratio of 38.4 dB. In this simulation, echoes from diffuse scattering medium surrounding the point scatterer were assumed to be random.

Fig. 7(a) shows the lateral profiles of non-normalized amplitudes of beamformed RF signals obtained without phase coherence factor (PCF) (red line), with PCF without subaperture beamforming (green line), and with PCF with 6 subapertures (blue line). As shown in Fig. 7, the peak echo amplitude obtained with PCF without subaperture beamforming is slightly decreased by the increase of the phase variance resulting from random signals. Such random signals are suppressed by subaperture beamforming before evaluation of PCF, and the suppression of the peak amplitude is avoided.

Fig. 7(b) shows the lateral profiles of normalized amplitudes. By avoiding the suppression of the peak amplitude, the width at half-maximum of the profile obtained with PCF with subaperture beamforming is found to be decreased slightly. This phenomenon can be considered as follows: When the location of the focal point coincides with that of the scatterer (corresponding to the peak of the lateral profile in Fig. 7), the phases of all echo signals are the same and the phase variance is zero if there is no noise. Therefore, all the noise components work to increase the phase variance. In other words, the phase variance is purely dependent on the random signals.

On the other hand, when the location of the focal point does not coincide with that of the scatterer, the phase variance is dependent on both the geometrical mismatch between the focal point and the scatterer and the random signals. Therefore, the increase of the phase variance caused by noise would be smaller than that at the peak of the lateral profile. As a result, a larger suppression of the echo amplitude resulting from the random signals occurs at the peak of the lateral profile, and the width at half-maximum increases, as shown in Fig. 7(b), when subaperture beamforming is not used.

In Fig. 4(b), although amplitude ratio r_a obtained with non-overlapping subapertures was increased by decreasing the number of non-overlapping subapertures, the lateral spatial resolution w_l was degraded when the number of subapertures was less than 8. By reducing the number of subapertures, a greater number of elements could be used

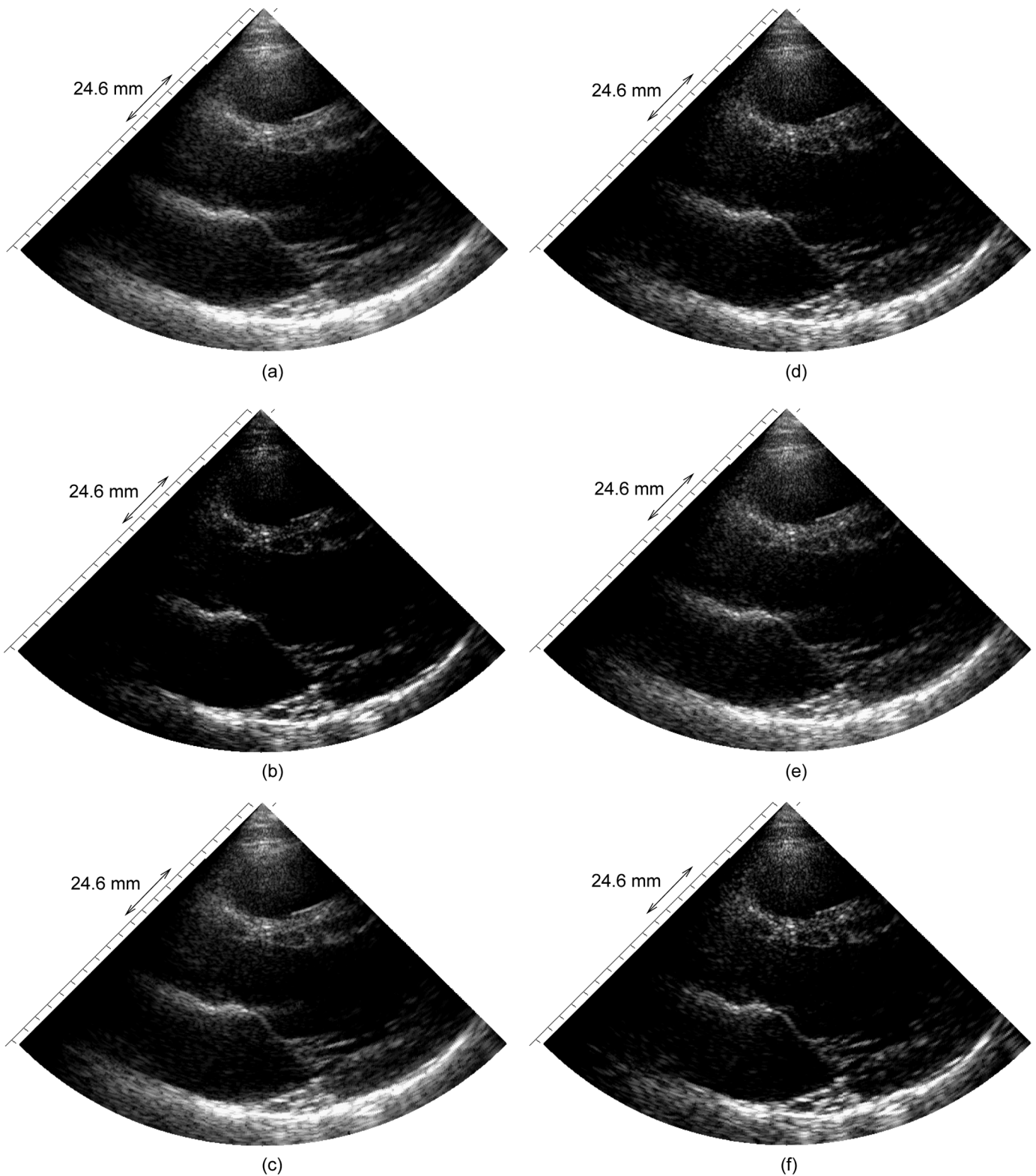


Fig. 6. B-mode images of a 26-year-old healthy male: (a) without the phase coherence factor, (b) with the conventional phase coherence factor, (c) with the controlled phase coherence factor ($\gamma = 0.5$), (d) with the phase coherence factor with 4 non-overlapping subapertures (24 elements/subaperture), (e) with the phase coherence factor estimated by 4 elements, and (f) with the phase coherence factor with 73 overlapping subapertures (24 elements/subaperture).

for subaperture beamforming, and greater suppression of out-of-focus echoes could be realized. Therefore, the phase coherence factor of an echo from a diffuse scattering medium could be estimated more correctly, and speckle echoes

were enhanced (corresponding to the increased amplitude ratio r_a and the reduced mean over standard deviation μ/σ). Spatial resolution was also improved (corresponding to small w_l) by more suppression of out-of-focus echoes

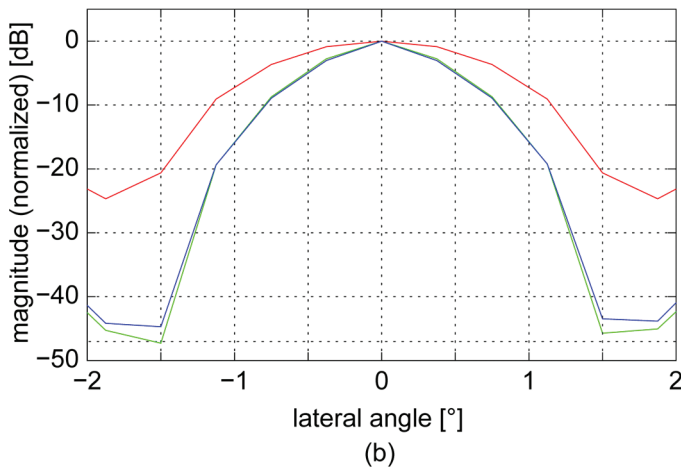
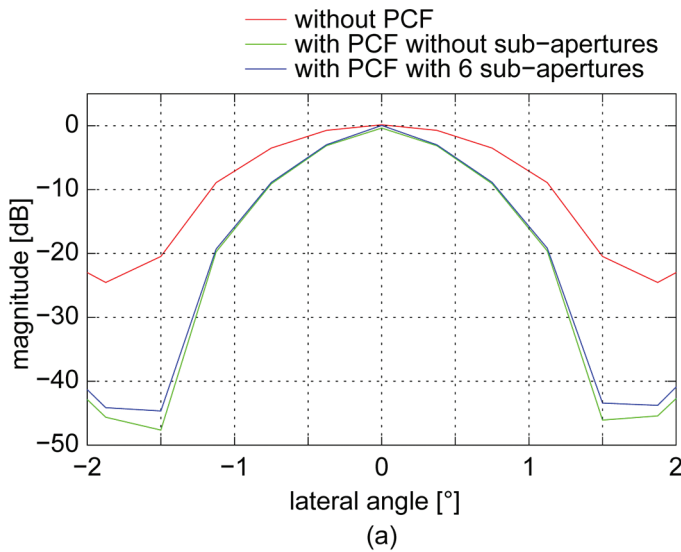


Fig. 7. (a) Non-normalized and (b) normalized lateral profiles of amplitude of an echo from a point scatterer obtained by simulation experiment.

by wider subapertures. The reason for the degradation of the spatial resolution at numbers of subapertures of less than 8 was considered to be that a small number of beamformed RF signals was not sufficient to obtain a statistically stable estimate of phase variance. However, the change in spatial resolution $\{w_l\}$ at numbers of subapertures of less than 8 is small, and such a small difference may be an error. Therefore, the spatial resolution w_l was evaluated at a different range distance of 61 mm, as shown in Fig. 8. In Fig. 8, a similar tendency can be confirmed, i.e., the spatial resolution w_l is also degraded at numbers of subapertures of less than 8.

In the present study, the number of elements in each subaperture was fixed, not depending on the range distance. The degree of suppression of out-of-focus echoes, which is achieved by the same number of elements (size) of a subaperture, would depend on the range distance even when the distance between the location of a scatterer (source of the out-of-focus echo) and the focal point is same. Therefore, it would be effective to change the subaperture size depending on the range distance to ob-

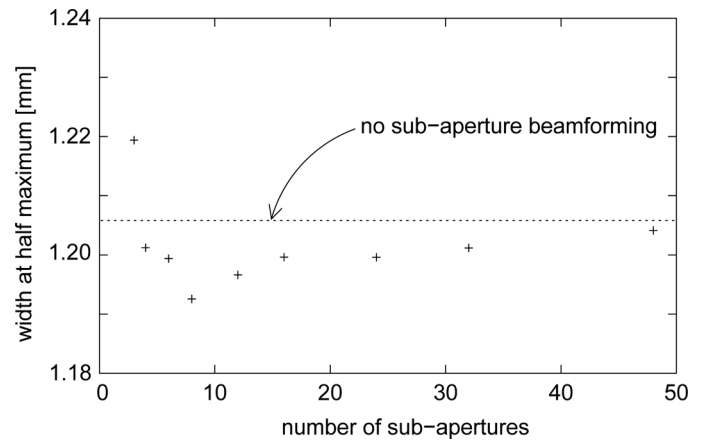


Fig. 8. Spatial resolution w_l at a range distance of 61 mm obtained with non-overlapping subapertures.

tain spatially homogeneous effects of subaperture beamforming. However, the variable subaperture has not been examined in the present study because the homogeneity of the image quality was not the main scope of the present study.

In delay-and-sum beamforming in each subaperture, the subsample time delay τ_s was compensated by multiplying the complex received signal $g_i(t)$ by $\exp(j2\pi f_0 \tau_s)$. In the present study, f_0 was set at 3 MHz, which was almost the center frequency of the received RF echo, whereas the nominal center frequency of the phased array probe was 3.75 MHz. As described in [30], [31], the center frequency of the received RF echo can vary by ultrasonic frequency-dependent attenuation, interference among echoes, etc. Although more computation is required, the estimation of the actual center frequency of the received RF echo would realize more accurate beamforming and estimation of the phase coherence factor.

Furthermore, although speckle echoes can be more visualized by subaperture beamforming, ultrasound imaging with the phase coherence factor increases the distance in intensity between echoes from specular and diffuse scatterers. In future work, it would also be necessary to investigate a more suitable method than the conventional log compression technique to appropriately show ultrasound images weighted by the phase coherence factors to physicians in clinical situation.

V. CONCLUSIONS

To realize high-frame-rate echocardiography, parallel beamforming has been introduced; however, spatial resolution was degraded by the use of unfocused transmit beams. Although the phase coherence factor is feasible for improvement of spatial resolution, speckle echoes from a diffuse scattering medium are suppressed. In the present study, a strategy for estimating the phase coherence factor has been presented for improvement of spatial resolution in high-frame-rate echocardiography and for avoiding suppression of speckle echoes. One of the reasons for reduc-

tion of the phase coherence factor estimated for a weak echo from a diffuse scattering medium was interference of echoes. Therefore, by using subaperture beamforming, a weak echo from a focal point in a diffuse scattering medium was enhanced, and the phase variance of echo signals received by individual transducer elements was reduced. As a result, suppression of speckle echoes could be successfully avoided without degradation of spatial resolution.

APPENDIX

RELATIONSHIP BETWEEN VARIANCE OF ESTIMATE AND NUMBER OF DATA

Let us define the phase of the RF echo signal received by the i th transducer element or subaperture ($i = 0, 1, \dots, K - 1$) by ϕ_i . There would be some degree of correlation between the phases evaluated from echo signals received by individual transducer elements, which are scattered by diffuse scattering medium. However, in this theoretical consideration, the phases of echo signals are assumed to be independent to simply explain the relationship between the number of phase data and the estimated phase variance. The measured phase includes random noise, which is assumed to obey the normal distribution. Let us also define the population mean and standard deviation of the measured phase ϕ_i by μ_ϕ and σ_ϕ . Under such conditions, the Cramér–Rao lower bound CLRB(σ_ϕ) in estimation of the population standard deviation σ_ϕ is expressed as [32], [33]

$$\text{CRLB}(\sigma_\phi^2) = \frac{1}{K \times E_i \left[\left\{ \frac{\partial}{\partial(\sigma_\phi^2)} \ln p(\phi_i) \right\}^2 \right]}, \quad (3)$$

where $E[\cdot]$ represents the expectation operator, and $p(\phi)$ is the probability density function of the measured phase ϕ_i , which is expressed as

$$p(\phi) = \frac{1}{\sqrt{2\pi\sigma_\phi^2}} \exp \left\{ -\frac{(\phi - \mu_\phi)^2}{2\sigma_\phi^2} \right\}. \quad (4)$$

Eq. (3) can be modified as follows:

$$\begin{aligned} \text{CRLB}(\sigma_\phi^2) &= \frac{1}{K \times E_i \left[\left\{ \frac{\partial}{\partial(\sigma_\phi^2)} \left(-\frac{1}{2} \ln(2\pi\sigma_\phi^2) - \frac{1}{2\sigma_\phi^2} (\phi_i - \mu_\phi)^2 \right) \right\}^2 \right]} \\ &= \frac{1}{E_i \left[\left\{ -\frac{1}{2\sigma_\phi^2} + \frac{1}{2\sigma_\phi^4} (\phi_i - \mu_\phi)^2 \right\}^2 \right]} \\ &= \frac{1}{K \int_{-\infty}^{\infty} \left(\frac{(\phi - \mu_\phi)^2}{2\sigma_\phi^4} - \frac{1}{2\sigma_\phi^2} \right)^2 \frac{1}{\sqrt{2\pi\sigma_\phi^2}} \exp \left\{ -\frac{(\phi - \mu_\phi)^2}{2\sigma_\phi^2} \right\} d\phi} \\ &= \frac{2\sigma_\phi^4}{K}. \end{aligned} \quad (5)$$

As described previously, the variance $\text{CRLB}(\sigma_\phi^2)$ in the estimation of the phase variance σ_ϕ^2 can be reduced by increasing the number of elements or subapertures K .

REFERENCES

- [1] G. R. Sutherland, M. J. Stewart, K. W. Groundstroem, C. M. Moran, A. Fleming, F. J. Guell-Peris, R. A. Riemersma, L. N. Fenn, K. A. Fox, and W. N. McDicken, "Color Doppler myocardial imaging: A new technique for the assessment of myocardial function," *J. Am. Soc. Echocardiogr.*, vol. 7, no. 5, pp. 441–458, 1994.
- [2] H. Kanai, H. Hasegawa, N. Chubachi, Y. Koiwa, and M. Tanaka, "Noninvasive evaluation of local myocardial thickening and its color-coded imaging," *IEEE Trans. Ultrason. Ferroelectr. Freq. Control*, vol. 44, no. 4, pp. 752–768, 1997.
- [3] A. Heimdal, A. Støylen, H. Torp, and T. Skjarpe, "Real-time strain rate imaging of the left ventricle by ultrasound," *J. Am. Soc. Echocardiogr.*, vol. 11, no. 11, pp. 1013–1019, 1998.
- [4] G. R. Sutherland, G. D. Salvo, P. Claus, J. D'hooge, and B. Bijnens, "Strain and strain rate imaging: A new approach to quantifying regional myocardial function," *J. Am. Soc. Echocardiogr.*, vol. 17, no. 7, pp. 788–802, 2004.
- [5] H. Kanai, "Propagation of vibration caused by electrical excitation in the normal human heart," *Ultrasound Med. Biol.*, vol. 35, no. 6, pp. 936–948, 2009.
- [6] H. Kanai and M. Tanaka, "Minute mechanical-excitation wave-front propagation in human myocardial tissue," *Jpn. J. Appl. Phys.*, vol. 50, no. 7, art. no. 07HA01, 2011.
- [7] D. P. Zipes and E. Braunwald, *Braunwald's Heart Disease: A Textbook of Cardiovascular Medicine*, Philadelphia, PA: Elsevier, 2005.
- [8] A. M. Katz, *Physiology of the Heart*, Philadelphia, PA: Lippincott Williams and Wilkins, 2001.
- [9] J. Cheng and J.-y. Lu, "Extended high frame rate imaging method with limited diffraction beams," *IEEE Trans. Ultrason. Ferroelectr. Freq. Control*, vol. 53, no. 5, pp. 880–899, May 2006.
- [10] P. M. Morse and K. U. Ingard, *Theoretical Acoustics*, Princeton, NJ: Princeton University Press, 1968.
- [11] J. F. Greenleaf, "Computerized tomography with ultrasound," *Proc. IEEE*, vol. 71, no. 3, pp. 330–337, 1983.
- [12] K. Nagai, "A new synthetic-aperture focusing method for ultrasonic B-scan imaging by the Fourier transform," *IEEE Trans. Sonics Ultrason.*, vol. SU-32, no. 4, pp. 531–536, 1985.
- [13] M. Couade, M. Pernot, M. Tanter, E. Messas, A. Bel, M. Ba, A.-A. Hagege, and M. Fink, "Ultrafast imaging of the heart using circular wave synthetic imaging with phased arrays," in *Proc. IEEE Ultrasonics Symp.*, 2009, pp. 515–518.
- [14] H. Hasegawa and H. Kanai, "High-frame-rate echocardiography using diverging transmit beams and parallel receive beamforming," *J. Med. Ultrasound*, vol. 38, no. 3, pp. 129–140, 2011.
- [15] J. Provost, T. H. Nguyen, D. Legrand, S. Okrasinski, A. Costet, A. Gambhir, H. Garan, and E. E. Konofagou, "Electromechanical wave imaging for arrhythmias," *Phys. Med. Biol.*, vol. 56, no. 22, pp. L1–L11, 2011.
- [16] L. Tong, H. Gao, H. F. Choi, and J. D'hooge, "Comparison of conventional parallel beamforming with plane wave and diverging wave imaging for cardiac applications: A simulation study," *IEEE Trans. Ultrason. Ferroelectr. Freq. Control*, vol. 59, no. 8, pp. 1654–1663, 2012.
- [17] H. Hasegawa and H. Kanai, "High frame rate echocardiography with reduced sidelobe level," *IEEE Trans. Ultrason. Ferroelectr. Freq. Control*, vol. 59, no. 11, pp. 2569–2575, 2012.
- [18] M. Tanter, J. Bercoff, L. Sandrin, and M. Fink, "Ultrafast compound imaging for 2-D motion vector estimation: Application to transient elastography," *IEEE Trans. Ultrason. Ferroelectr. Freq. Control*, vol. 49, no. 10, pp. 1363–1374, 2002.
- [19] J. Bercoff, S. Chaffai, M. Tanter, L. Sandrin, S. Catheline, M. Fink, J.-L. Gennisson, and M. Meunier, "In vivo breast tumors detection using transient elastography," *Ultrasound Med. Biol.*, vol. 29, no. 10, pp. 1387–1396, 2003.
- [20] J. Bercoff, M. Tanter, and M. Fink, "Supersonic shear imaging: A new technique for soft tissues elasticity mapping," *IEEE Trans. Ultrason. Ferroelectr. Freq. Control*, vol. 51, no. 4, pp. 396–409, 2004.

- [21] H. Hasegawa and H. Kanai, "Simultaneous imaging of artery-wall strain and blood flow by high frame rate acquisition of RF signals," *IEEE Trans. Ultrason. Ferroelectr. Freq. Control*, vol. 55, no. 12, pp. 2626–2639, 2008.
- [22] G. Montaldo, M. Tanter, J. Bercoff, B. Nicolas, and M. Fink, "Coherent plane-wave compounding for very high frame rate ultrasonography and transient elastography," *IEEE Trans. Ultrason. Ferroelectr. Freq. Control*, vol. 56, no. 3, pp. 489–506, 2009.
- [23] I. K. Holfort, G. Fredrik, and J. A. Jensen, "Broadband minimum variance beamforming for ultrasound imaging," *IEEE Trans. Ultrason. Ferroelectr. Freq. Control*, vol. 56, no. 2, pp. 314–325, 2009.
- [24] J. Synnevåg, A. Austeng, and S. Holm, "Adaptive beamforming applied to medical ultrasound imaging," *IEEE Trans. Ultrason. Ferroelectr. Freq. Control*, vol. 54, no. 8, pp. 1606–1613, 2007.
- [25] J. Camacho, M. Parrilla, and C. Fritsch, "Phase coherence imaging," *IEEE Trans. Ultrason. Ferroelectr. Freq. Control*, vol. 56, no. 5, pp. 958–974, 2009.
- [26] H. Hasegawa and H. Kanai, "Avoiding suppression of speckle echoes in phase coherence imaging," *Proc. 2014 Spring Meeting Acoustical Society of Japan*, 2014, p. 488.
- [27] D. Hyun, G. E. Trahey, and J. J. Dahl, "Efficient strategies for estimating spatial coherence on matrix probes," *2012 IEEE Int. Ultrasonics Symp. Proc.*, pp. 117–120, 2012.
- [28] J. J. Dahl and T. J. Feehan, "Direction of arrival filters for improved aberration estimation," *Ultrason. Imaging*, vol. 30, no. 1, pp. 1–20, 2008.
- [29] P. Li and M. Li, "Adaptive imaging using the generalized coherence factor," *IEEE Trans. Ultrason. Ferroelectr. Freq. Control*, vol. 50, no. 2, pp. 128–141, 2003.
- [30] T. Loupas, J. T. Powers, and R. W. Gill, "An axial velocity estimator for ultrasound blood flow imaging, based on a full evaluation of the Doppler equation by means of a two-dimensional autocorrelation approach," *IEEE Trans. Ultrason. Ferroelectr. Freq. Control*, vol. 42, no. 4, pp. 672–688, 1995.
- [31] H. Hasegawa and H. Kanai, "Reduction of influence of variation in center frequencies of RF echoes on estimation of artery-wall strain," *IEEE Trans. Ultrason. Ferroelectr. Freq. Control*, vol. 55, no. 9, pp. 1921–1934, 2008.
- [32] H. Cramér, *Mathematical Methods of Statistics*, Princeton, NJ: Princeton University Press, 1946.
- [33] C. R. Rao, "Information and the accuracy attainable in the estimation of statistical parameters," *Bull. Calcutta Math. Soc.*, vol. 37, pp. 81–89, 1945.



Hideyuki Hasegawa was born in Oyama, Japan, in 1973. He received the B.E. degree from Tohoku University, Sendai, Japan, in 1996. He received the Ph.D. degree from Tohoku University in 2001. He is currently an associate professor in the Graduate School of Biomedical Engineering, Tohoku University. His research interest is medical ultrasonic imaging and measurements of tissue dynamics and viscoelasticity. Dr. Hasegawa is a member of the IEEE, the Acoustical Society of Japan, the Japan Society of Ultrasonics in Medicine, and the Institute of Electronics, Information, and Communication Engineers.



Hiroshi Kanai was born in Matsumoto, Japan, on November 29, 1958. He received a B.E. degree from Tohoku University, Sendai, Japan, in 1981, and M.E. and Ph. D. degrees, also from Tohoku University, in 1983 and in 1986, both in electrical engineering. From 1986 to 1988, he was with the Education Center for Information Processing, Tohoku University, as a research associate. From 1990 to 1992, he was a lecturer in the Department of Electrical Engineering, Faculty of Engineering, Tohoku University. From 1992 to 2001, he was an

associate professor in the Department of Electrical Engineering, Faculty of Engineering, Tohoku University. Since 2001, he has been a professor in the Department of Electronic Engineering, Graduate School of Engineering, Tohoku University. Since 2008, he has been also a professor in the Department of Biomedical Engineering, Graduate School of Biomedical Engineering, Tohoku University. Since 2012, he has been a dean of the Graduate School of Engineering, Tohoku University.

His current interests are in transcutaneous measurement of the heart wall vibrations and myocardial response to propagation of electrical potential and cross-sectional imaging of elasticity around atherosclerotic plaque with transcutaneous ultrasound for tissue characterization of the arterial wall.

Dr. Kanai is a member of the Acoustical Society of Japan, a fellow of the Institute of Electronics Information and Communication Engineering of Japan, a member of the Japan Society of Ultrasonics in Medicine, Japan Society of Medical Electronics and Biological Engineering, and the Japanese Circulation Society. Since 1998, he has been a member of Technical Program Committee of the IEEE Ultrasonics Symposium. Since 2008, he has been a member of the International Advisory Board of the International Acoustical Imaging Symposium. Since 2011, he has been a board member of the International Congress on Ultrasonics. Since 2012, he has been an editor of the *Journal of Medical Ultrasonics* and the *Japanese Journal of Medical Ultrasonics*. Since 2013, he has been an associate editor of the *IEEE Transactions on Ultrasonics, Ferroelectrics, and Frequency Control*.